ScienSage

Journal of Advanced Scientific Research

Available online through http://www.sciensage.info

ISSN
0976-9595
Research Article

SYNTHESIS, CHARACTERIZATION AND *IN VITRO* ANTITUBERCULAR AND ANTIMICROBIAL ACTIVITY OF Cu(II) AND Zn(II) COMPLEXES WITH TRIDENTATE LIGAND

Sakina Z Bootwala

Department of Chemistry, Wilson College, Mumbai, India

**Corresponding author: szbootwala@gmail.com*

ABSTRACT

Cu(II) and Zn(II) complexes were prepared with ethyl 2-{[(*E*)-(2-hydroxynaphthalen-1-yl)methylidene]amino}-4,5,6,7-tetrahydro-1-benzothiophene-3-carboxylate(HETBT-Np),a tridentate Schiff base ligand. Schiff base ligand was subjected to various spectroscopic investigations like NMR, IR, UV-Visible, and LCMS for structural determination, while complex geometry was proposed on the basis of FTIR, UV-Visible, ESR, XRD, TGA spectroscopy and measurement of molar conductivity, magnetic susceptibility, and elemental analysis. All the prepared compounds displayed *in vitro* antimicrobial activity against Drug Resistant Extended Spectrum β-Lactamase (ESBL), and Metallo β-lactamase (MBL) producing uropathogens and antitubercular activity against *Mycobacterium tuberculosis* (H37Rv strain). Metal complexes exhibited enhanced biological activity compared to parent Schiff base. Among the studied metal complexes, Cu (II) complex surfaced as the most active compound against all of the tested microbial strains.

Keywords: Metal complex, Schiff base, tridendate ligand, Metallo β-lactamase

1. INTRODUCTION

Metal complexes with tridentate and tetradentate ligands have created much interest in coordination chemistry. Schiff base complexes of transition metals have played a important role in the development of coordinaton chemistry. Several Schiff base metal complexes have been studied because of their industrial and biological applications. Heterocyclic compound are extensively distributed in nature and have versatile synthetic applicability and biological activity which implement the new approaches for the medicinal chemist to plan and organize towards the discovery of novel drugs [1]. Thiophene and its derivatives showed extensive significance in pharmaceutical field because of its varied biological and clinical applications [2, 3].

Aminothiophenes Schiff bases are comparatively less studied, mainly because of their instability, but suitable substitution like the introduction of carboxy-ethyl group not only makes them stable but also provides new coordination sites [4]. Schiff bases derived from naphthaldehyde or salicylaldehyde are easy to prepare but show chemical instability and undergo tautomerization; hence careful studies are required. Only 52% of multidrug-resistant tuberculosis (MDR-TB) cases were cured globally [5]. Like *M. tuberculosis*, gram-negative bacteria are also evolving as drug resistance strains especially Extended Spectrum-β-lactamase (ESBL) and Metallo-β-lactamase (MBL) producing organisms. Repeated or lengthy courses of antibiotics and unhygienic conditions are some of the common cause for the recent emergence of these multidrug-resistant bacterial strains [6]. The present antibiotics seem insufficient to cover the medical need in the near future which highlights the demand for more effective drugs against these drug-resistant strains.

In continuation to our previous studies, we report the synthesis of aminothiophene Schiff base derived from 2-hydroxy-1-naphthaldehyde and its transition metal complexes and their antimicrobial activity against ESBL and MBL gram-negative bacteria and *M. tuberculosis*.

2. EXPERIMENTAL

2.1. Material and methods

Analytical grade chemicals with purified and distilled solvents were used during the experiment. The proton NMR spectra of Schiff base ligand was recorded on Varian-NMR-Mercury 300 MHz instrument using TMS as internal standard and DMSO-d^6 as a solvent. Mass spectra (MS) of Schiff base was recorded on BRUKER ESQUIRE HCT spectrometer. The elemental analysis was carried out by Thermo Finnigan CHNS(O) Analyzer and metal content was determined by ARCOS, ICP-

Atomic Emission Spectrometer. Chlorine percentage was estimated by Volhards method [7]. Molar conductance measurement was done on an ELICO Digital conductivity meter Model CM-180 at room temperature in DMF (10^{-3} M solution). Powder X-ray study was carried out using PAN analytical X-ray diffractometer. For IR spectral analysis Perkin Elmer Model 1600 FTIR Spectrophotometer was used. Thermogravimetric analysis of the selected copper complex was carried out using PERKIN ELMER diamond thermogravimetric analyzer. UV-Vis-Jasco Spectrophotometer Model V-630 was employed for electronic spectral analysis. Gouy balance was used for magnetic susceptibility measurements along with $Hg[Co(SCN)_4]$ as calibrant. Diamagnetic corrections were calculated using Pascal's constants.

2.2. Anti-tuberculosis Screening

For the determination of antitubercular activity non-toxic Microplate Alamar Blue Assay (MABA) method was employed. *M. tuberculosis* (H37Rv strain) ATCC No-27294 was used as test microorganism. Mixture of sterile de-ionized water (200 µl) and Middlebrook 7H9 broth (100 µl) with a serial dilution of compounds were added directly to the sterile 96 well plate. The compounds were tested at the concentrations of 100, 50, 25, 12.5, 6.25, 3.12, 1.6 and 0.8 µg/ml. These plates were covered and sealed using paraffin and kept for incubation at 37°C for five days. After 5 days, freshly prepared 1:1 mixture of Almar Blue reagent and Tween 10% and Tween 80% (25µl) was added to the plate and again incubated for another one day. Antitubercular activity was correlated to the disappearance of pink color at a minimum concentration in the well termed as MIC (Minimum Inhibitory Concentration) [8].

2.3. Antimicrobial Screening

Clinically characterized ESBL and MBL producing gram-negative uropathogens were collected from the local hospitals and pathological laboratories in Mumbai [9]. Namely five ESBL and five MBL isolates of each of genera, *Klebsiella*, *Escherichia*, *Pseudomonas*, *Proteus,* and *Citrobacter*) were used in antimicrobial activity evaluation (Table 5). Kirby Bauer and agar well diffusion method was employed to study antibacterial activity. HPLC grade DMSO was used as a solvent, in which all compounds were dissolved to obtain a final concentration of 25 µg/ml. Brain Heart infusion (BHI) broth of 10 ml was used to inoculate bacterial culture and incubated at 37°C for one day. Sterile and cooled 20 ml of molten Mueller and Hinton agar butt was seeded with 0.4 ml test culture (0.1 O.D. at 540 nm) and poured into a 9cm diameter Petri plate. Wells of diameter 80mm were punched in each plate after solidification of the medium. These wells were poured with 50µl of the test compound and incubated at 37°C for one day to develop the zones of inhibition. Control wells were set up using 50 µl of DMSO for each isolate. The experiment was repeated in three sets and the results were reported as mean ± Standard Deviation (SD).

2.4. Synthesis of ligand

The Schiff base ligand ethyl 2-{[(*E*)-(2-hydroxynaphthalen-1-yl)methylidene]amino}-4,5,6,7-tetrahydro-1-benzothiophene-3-carboxylate (HETBT-Np) was prepared from the condensation of ethyl-2-amino-4,5,6,7-tetrahydrobenzo[*b*]thiophene-3-carboxylate (ETBT) [10] and naphthaldehyde as per reaction scheme (Figure 1). Equimolar proportion (0.01 M) of ETBT (2.247 g) and 2-hydroxy-1-naphthaldehyde (1.722 g) in dry ethanol (20 ml) was condensed in a water bath for 4 hours. The reaction mixture was poured into ice water, to obtain orange colored solid Schiff base. This solid was filtered, washed and dried. Further, it was recrystallized from ethanol.

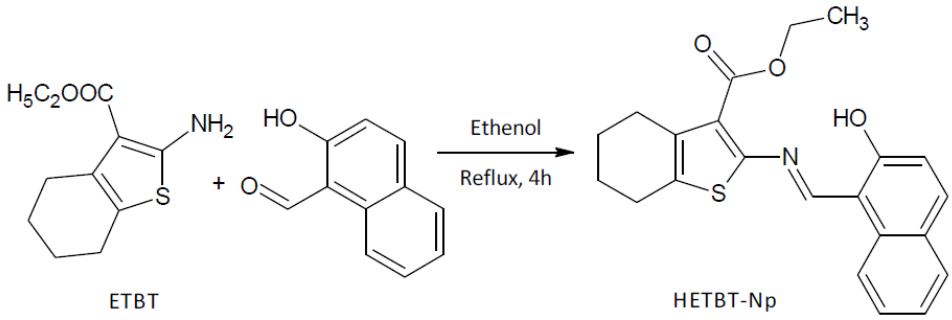

Fig. 1: Reaction Scheme

2.5. Synthesis of metal complexes

The Schiff base metal complexes were prepared by refluxing the ethanolic solution of metal chlorides with warm ethanolic solutions of ligand in 1:1 molar ratio for Cu(II) and Zn(II) complexes at the pH of 6.5 for 5-6 hours. The complex formed was filtered, washed sequentially with aqueous ethanol and ether. Finally, the complex was dried in vacuum over P_4O_{10}. Formation of the complexes can be symbolized as follows,

MCl_2 + HETBT-Np → [M(ETBT-Np)Cl] + HCl

M = Cu(II) and Zn(II)

3. RESULTS AND DISCUSSION

3.1. Characterization of Schiff base

Elemental analysis of Schiff base envisages 1:1 molar condensation of ETBT and 2-hydroxy-1-naphthaldehyde which is further confirmed by NMR & IR spectra [11].

3.2. ^{1}H NMR Spectra

^{1}H NMR spectra of ETBT showed multiplets in the range of 1.63-2.56 δ attributed to aromatic protons of cyclohexane ring. Triplet at 1.19-1.23 δ and quartet at 4.08-4.15 δ can be attributed to methyl and methylene protons respectively. The downfield singlet at 7.18 δ can be assigned to amino protons. In the proton NMR spectrum of HETBT-Np singlet due to amino protons disappears and new singlet due to azomethine protons (–CH=N–) at 9.35 δ appears which confirm the condensation ETBT and 2-hydroxy-1-naphthaldehyde. The proton NMR spectrum of HETBT-Np exhibits multiplets in the range of 1.74-2.66 δ and 7.12-8.37 δ attributed to aromatic protons of cyclohexane and aromatic protons of naphthaldehyde respectively. Signals for methyl and methylene protons were observed at 1.29-1.33 δ and 4.25-4.32 δ respectively. Phenolic proton (–OH) of naphthaldehyde exhibited a most downfield peak at 14.45 δ.

3.3. FTIR and Mass Spectra

FTIR spectra of Schiff base exhibited broad absorption bands at 3200-3000 cm^{-1} due to a phenolic hydroxyl group (-OH), another strong band at 1695 cm^{-1} and 1601 cm^{-1} were assigned to ester carbonyl (C=O) and azomethine group (C=N) respectively. A medium intensity band due to (C=S) vibration was observed at 635 cm^{-1}. Significant IR bands are given in Table 5. LCMS spectra of ligand exhibited molecular ion peak [M+1] at m/z 380 (calculated m/z 379) [11].

3.4. Electronic Spectra

Schiff bases derived from the condensation of aromatic aldehydes having ortho hydroxyl group and primary amines exhibits either O··H--N or O--H··N type of intramolecular hydrogen bonding giving rise to an enol-imine form of tautomerism. Such compounds can be differentiated using electronic spectroscopy [11]. The electronic absorption spectrum of the Schiff base in DMF showed strong bands at 250 nm and 318 nm for $\pi \rightarrow \pi^*$ and $n \rightarrow \pi^*$ transitions respectively. These bands were attributed to the phenol-imine form of Schiff base. Further, the absence of a band at 400 nm due to quinine-amine form confirms the presence of phenol-imine form.

3.5. *Characterization of metal complex*

The ligand formed well-defined, stable and colorful complexes with transition metal chlorides. All the complexes were partly soluble in methanol and ethanol and highly soluble in DMF and DMSO. Analytical data of the complexes are in good agreement with their proposed formulation. Physico-chemical data (Table 1) supports the 1:1 metal-to-ligand stoichiometry of copper and zinc complexes.

Table 1: Physico-chemical characteristics of metal complexes

Complex	Colour	F.W.	Elemental analysis (%) found (calc.)						Molar conductance in DMF (Ω^{-1} cm^2 mol^{-1})
			C	H	N	S	Cl	M	
HETBT-Np	Orange	379.47	70.11 (69.57)	5.45 (5.53)	3.78 (3.69)	8.26 (8.43)	-	-	-
[Cu(ETBT-Np)Cl]	Saddle brown	477.46	55.70 (55.29)	4.23 (4.19)	2.25 (2.93)	6.93 (6.70)	7.31 (7.43)	13.49 (13.31)	1.80
[Zn(ETBT-Np)Cl]	Purple	479.33	54.67 (55.08)	4.24 (4.17)	2.82 (2.92)	6.73 (6.68)	7.25 (7.40)	13.95 (13.65)	1.10

3.6. FTIR spectra

The IR spectra of the metal complexes were compared with the IR spectra of the free ligand, for determining the sites of coordination and are given in Table-2. The band at 3000-3200 cm^{-1} due to phenolic -OH was absent in the IR spectra of all metal complexes suggesting the participation of phenolate oxygen through deprotonation [12]. The sharp peak at 1695 cm^{-1} due ester carbonyl was shifted to lower frequency suggesting the participation of carbonyl oxygen in complex formation [13]. The stretching vibration at 1601 cm^{-1} due to azomethine group (-C=N-) was shifted to lower frequency indicating [14] linkage of azomethine nitrogen to the metal atom. Shifting of phenolic oxygen (C-O) band at 1291 cm^{-1} to higher wavelength further supports the deprotonation of phenolic –OH group. The SH stretching absorption of free ligand at 635 cm^{-1} remained unaffected after complexation indicating non-participation of thiophene sulfur in coordination [15]. Additionally, weak non-ligand bands were observed at 514-510 cm^{-1}, and 416-407 cm^{-1}, which were assigned to the υ(M-O) stretching and υ(M-N) vibrations respectively . It is evident that the ligand acts as a monobasic tridentate ligand and binds to the metal ion through azomethine nitrogen, phenolate oxygen, and carbonyl oxygen.

Table 2: Important IR spectral bands

Compound	Tentative Assignments (cm^{-1})						
	υ(O-H)	υ(C=O)	υ(C=N)	υ(C-O)	υ(C-S)	υ(M←O)	υ(M←N)
HETBT-Np	3200-3000	1695	1601	1291	635	-	-
[Cu(ETBT-Np)Cl]	-	1637	1571	1305	634	514	412
[Zn(ETBT-Np)Cl]	-	1632	1569	1312	635	510	416

Table 3: Electronic spectral bands and Magnetic moment

Complex	Absorption bands (cm^{-1})	Tentative assignment	Magnetic moment (BM)
[Cu(ETBT-Np)Cl]	40486	INCT	1.88
	33898	INCT	
	31646	INCT	
	19920	$^2B_{1g} \rightarrow {}^2A_{1g}$	

3.7. Molar Conductance, Electronic Spectra, and Magnetic Susceptibility

Metal complexes showed negligible molar conductance values (Table 1) which highlights the non-electrolytic character of the metal complexes. The UV-Visible spectra of the metal complexes in DMF exhibited slightly redshifting in π→π* and n→π* ligand transitions indicating coordination of ligand to a metal ion (Table-3). The UV-visible spectra of [Cu(ETBT-Np)Cl] complex exhibited mainly three intraligand charge transfer bands (INCT) and a d-d transition corresponding to $^2B_{1g} \rightarrow {}^2A_{1g}$ which is characteristic of square-planar geometry. The square planar geometry of [Cu(ETBT-Np)Cl] complex is supported by magnetic moment value of 1.88 BM and absence of band below of 10000 cm^{-1} for tetrahedral geometry. In case of [Zn(ETBT-Np)Cl] complex, due to completely filled d^{10} configuration no d-d transitions were observed. Based on diamagnetic nature and empirical formulae supported by elemental analysis a tetrahedral structure is proposed for [Zn(ETBT-Np)Cl] complex [16].

3.8. ESR spectra

The powder EPR spectra of the [Cu(ETBT-Np)Cl] complex (Figure 2) was recorded in a solid state at room temperature in the X-band region. The observed g values were $g\| = 2.1283$, $g\perp = 2.0268$ and $g_{av} = 2.0606$ which follows the order as $g| > g\perp > g_e$ which is similar to ground state $dx^2\text{-}y^2$ configuration [17]. The empirical factor $f = g|| / A||$ is often considered as an index of tetrahedral distortion in square planar complexes and equatorial plane distortion in octahedral or square-pyramidal complexes. The ratio of 105-135 indicates distortion in square planar complex and 150-250 denotes distortion in octahedral or square-pyramidal complexes. However, the observed g|| / A|| quotient for the

complexes is 134 which is indicative of distorted square-planar geometry [18]. The calculated inplane σ covalency parameter (α^2_{Cu}) given as $\alpha^2_{Cu} = -(A\parallel/0.036) + (g\parallel - 2.002) + 3/7 (g\perp - 2.002) + 0.04$ is 0.62, which is indicative of the covalency in the metal-ligand bonding.

The axial symmetry parameter (G), given as $G = (g\parallel - 2/g\perp - 2)$ was calculated to 4.79. This (G) parameter points towards the formation of monomeric copper complexes and the parallel alignment of local tetragonal axes with negligible exchange interaction [19].

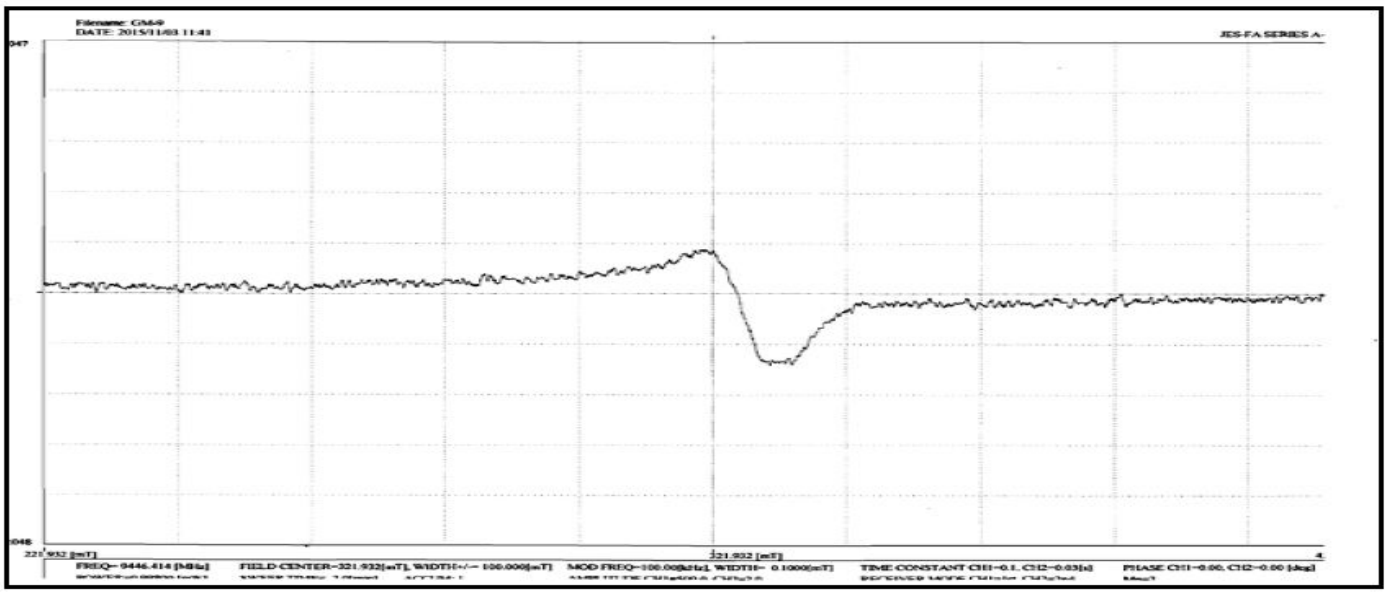

Fig. 2: ESR spectra of [Cu(ETBT-Np)Cl] complex

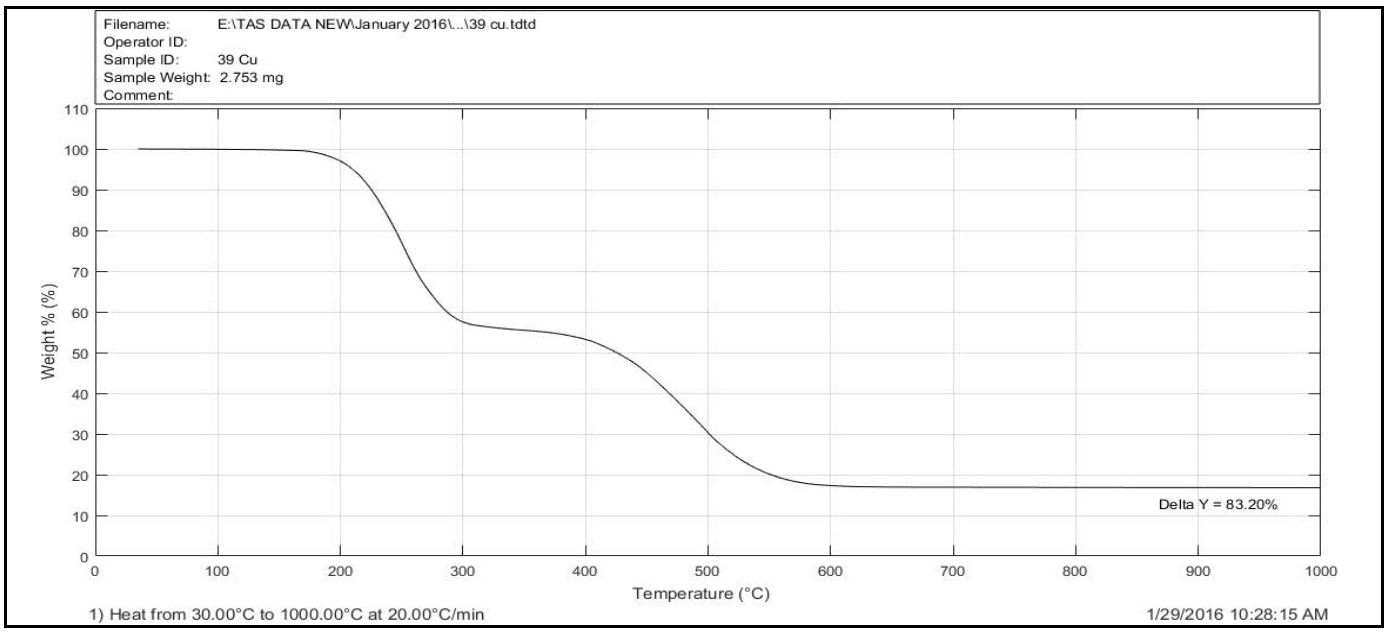

Fig. 3: Thermogram of [Cu(ETBT-Np)Cl] complex

3.9. Thermogravimetric Analysis

The thermal decomposition of the [Cu(HETBT-Np)Cl] complex was examined under a nitrogen atmosphere by TG method from room temperature to 1000°C. The stages of decomposition, decomposition products and the observed and calculated percentage mass loss of the complex are depicted in Table 4. The thermogram of Cu(II) metal complex (Figure 3) is stable up to 170°C, gradually decomposing to CuO over 600°C. First stage decomposition occurred in the temperature range 170 to

310°C was assigned to the loss of amino-substituted aminothiophene moiety. Second stage decomposition was observed from 320°C which continued up to 600°C accounting for the loss of naphthaldehyde group and a bonded chlorine atom. The horizontal plateau was observed over 600°C at the end of second stage decomposition which corresponds to the final residue of CuO.

Table 4: Thermal decomposition scheme for [Cu(HETBT-Np)Cl] complex

Complex	Temperature range °C	Weight loss % theo. (exp.)	Decomposition product
[Cu(ETBT-Np)Cl]	170-310	43.83 (43.29)	$C_{11}H_{13}O_2S$
	320-600	39.51 (39.60)	$C_{11}H_7N$+(Cl)
	>615 (residue)	16.66 (17.11)	CuO

3.10. X-ray Analysis

The [Zn(ETBT-Np)Cl] complex was subjected to the powder X-ray diffraction technique. Powder X-ray diffraction pattern showed sharp intense peaks suggesting the crystalline nature of all the complexes (Figure-4). The X-ray pattern was scanned between 2θ ranging from 10° to 90° at the wavelength of 1.5406 Å. Crystal lattice parameters were calculated using Rietveld refinement technique [20]. The complex was found to belong from monoclinic system with space group $P12_1/c1$ [21] having unit cell parameters such as a = 9.3364 Å, b = 14.8119 Å, c = 33.6668 Å, Z = 4, density = 2.044 g/cc and V = 4655.06 Å^3 with maximum reflection at 2θ = 19.4532° corresponding to interplanar distance of d = 4.5594 Å and β = 91.004°. The average grain size was calculated to 38 nm using Scherer's formula D = 0.9λ/βcosθ [22].

From spectral analysis and physico chemical data the structure of transition metal complexes can be proposed as shown in Figure5.

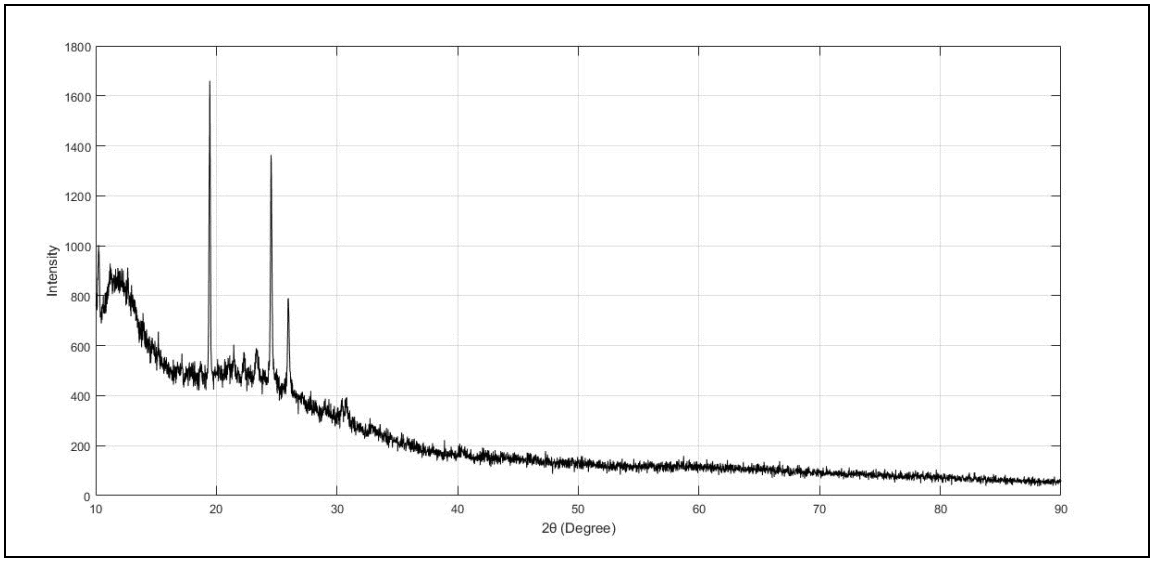

Fig. 4: XRD of [Zn(ETBT-Np)Cl]

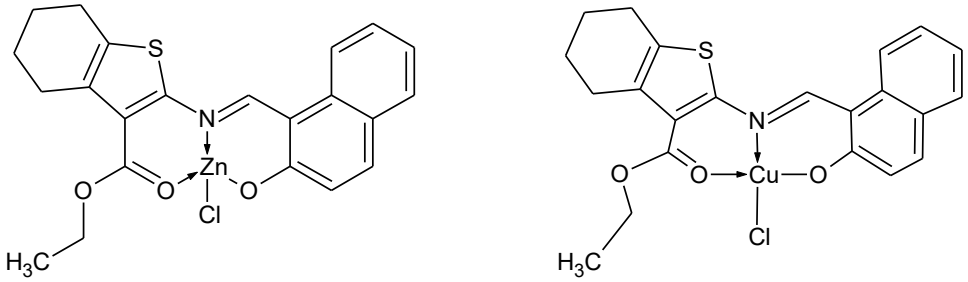

Fig. 5: Proposed structure of metal complexes

3.11. Antimicrobial activity

The antimicrobial activity of Schiff base and its Cu(II) and Zn(II) metal complexes have been explored against multiple drug resistant ESBL and MBL producing microbial isolates using DMSO as a solvent. The general resistance profile of these isolates against some common drugs is given in Table 5 and antimicrobial activity of tested compounds in the zone of inhibition (mm) is given in Table 6. The ligand itself has shown antimicrobial activity (11-15 mm) against some test isolates such as *Klebsiella pneumoniae-7* (Kp-7), *Pseudomonas aeruginosa* (85) and *Citrobacter amalonaticus* (135). Among the test compounds Cu(II) complex was found to be the most active compound (10-16 mm) exhibiting activity against all test isolates than Zn(II) complex. Test isolate *Klebsiella pneumoniae-7* (Kp-7), *Pseudomonas aeruginosa* (85) and *Citrobacter amalonaticus* (135) were sensitive to all compounds. *Citrobacter amalonaticus* (135) was the most sensitive to these compounds (12-18 mm). Test isolate *Klebsiella pneumoniae* (Kp) and *Proteus mirabilis* (607) were observed to be the most resistant microbial strains, only sensitive to copper complex. The enhanced activity of metal complexes compared to parent ligand is may be the effect of chelation due to which the overall permeability the specific complex is increased allowing the deeper penetration of the complex through the lipid layer of the microbial cell [23].

Table 5: Antibiotic resistance profile of ESBL and MBL uropathogens

Cultures code name	Full form	Antibiotic sensitivity test		
		Sensitive	Intermediate	Resistant
ESBL PRODUCERS				
Citro-2	*Citrobacter diversus-2*	AS, BA, CH, RC, TE	CI, CF	CF, PC, ZN, GM, AK, GF, TT, OX, RP, ZX, CB, NA, NX, AG, CU, CP, FG, PB
Ec- 10	*Escherichia coli-10*	CH, GM, AK, GF	PB, AS	BA, CF, PC, RC, CI, TE, ZN, TT, OX, RP, ZX, CB, NA, NX, AG, CU, CP, FG
Kp	*Klebsiella pneumoniae*	GM, AK	-	AS, BA, CF, PC, CH,RC, CI, TE, ZN, GF, TT, OX, RP, ZX, CB, NA, NX, AG, CU, CP, FG, PB
Kp-7	*Klebsiella pneumoniae- 7*	-	OX, TE	AS, BA, CF, PC, CH,RC, CI, ZN, GM, AK, GF, TT, RP, ZX, CB, NA, NX, AG, CU, CP, FG, PB
Pro- 7	*Proteus mirabilis-7*	CP, AS, PC, AK	RP, NA, CF, RC, GM, GF	BA, CH, CI, TE, ZN, TT, OX, ZX, CB, NX, AG, CU, FG, PB
MBL PRODUCERS				
85	*Pseudomonas aeruginosa*	AK, GF, PB	RC, CF, PC	AS, CI, TE, ZN, GM, TT, OX, RP, ZX, CB, BA, CH, NA, NX, AG, CU, CP, FG,
135	*Citrobacter amalonaticus*	CH, PB	AK	AS, BA, CF, PC, RC, CI, TE, ZN, GM, GF, TT, OX, RP, ZX, CB, NA, NX, AG, CU, CP, FG, CB, AS
220	*Escherichia coli*	CH, AK, GF	AS, ZN	BA, CF, PC, RC, CI, TE, GM, TT, OX, RP, ZX, CB, NA, NX, AG, CU, CP, FG, PB
607	*Proteus mirabilis*	-	CH, GM	AS, BA, CF, PC, RC, CI, TE, ZN, AK, GF, TT, OX, RP, ZX, CB, NA, NX, AG, CU, CP, FG, PB
618	*Klebsiella pneumoniae*	-	-	AS, BA, CF, PC, CH,RC, CI, TE, ZN, GM, AK, GF, TT, OX, RP, ZX, CB, NA, NX, AG, CU, CP, FG, PB

TT -Ticarcillin/clavulanic acid, OX- Oxytetracycline, RP - Ceftriaxone, ZX - Cefepime, CB - Cefuroxime, NA - Naladixic acid, NX- Norfloxacin, AG - Amoxycillin/clavulanic acid, CU - Cefadroxil, CP - Cefoperazone, FG- Ceftazidime, PB - Polymixin B, AS - Ampicillin, BA - Co-trimaxazole, CF -Cefotaxime, PC- Pipperacillin, CH - Chloramphenicol, RC - Ciprofloxacin, CI - Ceftizoxime, TE - Tetracycline, ZN - Ofloxacin, GM – Gentamicin, AK -Amikacin, GF - Gatifoxacin

Table 6: Antimicrobial activity

Cultures code name		Zone of Inhibition in mm		
		HETBT-Np	[Zn(ETBT-Np)Cl]	DMSO (solvent)
Citro-2	ESBL	0	0	0
Ec- 10		0	0	0
Kp		0	0	0
Kp-7		11	11	0
Pro- 7		0	0	0
85	MBL	13	12	0
135		15	16	0
220		0	0	0
607		0	14.5	0
618		0	11	0

Table 7: Antitubercular activity

Test compound	MIC (µg/ml)							
	100	50	25	12.5	6.25	3.12	1.60	0.80
*Streptomycin**	S	S	S	S	S	R	R	R
*Pyrazinamide**	S	S	S	S	S	S	R	R
*Ciprofloxacin**	S	S	S	S	S	S	R	R
HETBT-Np	S	S	R	R	R	R	R	R
[Ni(ETBT-Np)Cl]	S	S	R	R	R	R	R	R
[Co(ETBT-Np)$_2$]	S	S	R	R	R	R	R	R
[Cu(ETBT-Np)Cl]	S	S	S	R	R	R	R	R
[Zn(ETBT-Np)Cl]	S	S	S	R	R	R	R	R

** Standard, S - Sensitive, R - Resistant*

3.12. Antitubercular activity

All synthesized compounds displayed antitubercular activity against *M. tuberculosis* in presence of Pyrazinamide, Ciprofloxacin, and Streptomycin reference drugs (Table 7). Schiff base exhibited moderate antitubercular activity at MIC of 50 µg/ml. However copper and zinc complex showed enhanced activity (MIC of 25 µg/ml) compared to parent Schiff base. The improved activity of copper and zinc complex can attribute to the process of chelation. The coordination of copper/zinc atom with Schiff base may be forming a specific complex with cell wall protein having enhanced lipophilic character due to which it may have deep penetration within the host cell and interference in cell wall synthesis [24].

4. CONCLUSION

The Schiff base is prepared by condensation of ethyl-2-amino-4,5,6,7-tetrahydrobenzo[*b*]thiophene-3-carboxy - late and 2-hydroxy-1-naphthaldehyde and their transition metal complexes. Schiff base behaved as monobasic trident ligands coordinating through ester carbonyl, azomethine and phenolic group with the central metal atom. copper, and zinc metal complex were formed in 1:1 metal to ligand. The observed geometry for copper and zinc complex was distorted square planar and tetrahedral respectively. The biological activity of the metal complexes was found to increase than the parent Schiff base against ESBL & MBL uropathogens and *M. Tuberculosis*. Among the synthesized compounds copper complex displayed significant antimicrobial activity and copper and zinc complexes exhibited highest anti-tubercular activity. Overall, copper complex surfaced as the most active complex. Thus, there is future potential for the development of more active Schiff base complexes with high therapeutic value.

5. REFERENCES

1. Mishra R, Sharma PK, *Int J Eng Allied Sci.*, 2015; **1(1):**46-59.
2. Kolavi G, Hegde V, Khazi I, Gadad P, *Bioorg Med Chem.*, 2006; **14:**3069-3080.

3. Shah R, Prabhakar K, Verma S. *BMC Chemistry*, 2019; **13(54):**3-13.
4. Mohanan K, Nirmala Devi S, Murukan B. *Metal-Org. nano-Met. Chem.*, 2006; **36:**441-451.
5. Kumar M, Dutta, Saxena S, Singhal S. *J. Clin. Diagn. Res.,* 2015; **9(11)**:DC08-13.
6. Public Health England, Extended-spectrum beta-lactamases (ESBLs): guidance, data, analysis (2014); https://www.gov.uk/government/collections/extended-spectrum-beta-lactamases-esbls-guidance-data-analysis
7. Vogel AI., Textbook of quantitative chemical analysis. London: Longmans, Addison Wesley 1999.
8. Lourenço MC, De Souza MV, Pinheiro AC, Ferreira MD, Gonçalves RC, et al. *Arkivoc*, 2007; **15**:181-191.
9. Tariq M, Aruna K. *Br. Microbiol. Res. J.*, 2015; **5**:368-383.
10. Gewald K, Schinke E, Bottcher H. *Chem. Berr.*, 1966; **99**:94-100.
11. Bootwala SZ. *Journal of Interdisciplinary Cycle Research*, 2020; **XII (1):**6-15.
12. Devi SN, Mohanan K. *Asian. J. Chem.*, 2002; **14**:1678-1682.
13. Mohanan K, Devi SN. *Russian J. Coord. Chem.*, 2006; **32**:600-609.
14. Issa RM, Khedr AM, Rizk H. *Spectrochimica Acta A***,** 2006; **65:**206-214.
15. Aruna K, Bootwala SZ. *Int. J. Pharm. Bio. Sci*, 2012; **3**:1063-1074.
16. Rahim S, Antony A, Lukose G, Mohanan K, et al. *Oriental J. Chem.*,2015; **31(4)**:1949-1960.
17. Lekha A, Kanmaniraja K, Rajagopal G, Sivakumar D, Easwaramoorthi D. *Int. J. Chem. Pharmaceut. Sci.,* 2013; **4(2)**:48-54.
18. Borthakur R, Kumar A, De AK, Lal RA. *Arabian J. Chem.*, 2019; **12(8):**2192-2205.
19. Shanmugakala R, Tharmaraj P, Sheela CD, Anitha C. *Int. J. Inorg. Chem.*, 2012; **2012**:Article ID 301086, 7 pages
20. Rietveld HM. *Acta Crystallogr.*, 1967; **22:**151-152.
21. Lin ZE, Fan W, Gao F, Chino N, Yokoi T, Okubo T. *Cryst. Growth Des.*, 2006; **611**:2435-2437.
22. Patterson AL. *Physical Review*, 1939; **56**:978-982.
23. Sheikh J, Juneja H, Ingle V, Ali P, Hadda TB. *J. Saudi Chem. Soc.*, 2013; **17**:269-276.
24. Yamgar S, Nivid Y, Nalawade S, Mandewale M, Atram RG, Sawant SS. *Bioinorg. Chem. Appl.*, 2014; Article ID 276598;10 pages.